

**-Supporting Information-**

# Investigating the Multiple Roles of Polyvinylpyrrolidone for A General Methodology of Oxide Encapsulation

*Hang Sun,<sup>†</sup> Jiating He,<sup>†</sup> Jiangyan Wang,<sup>§</sup> Shuang-Yuan Zhang,<sup>‡</sup> Cuicui Liu,<sup>†</sup> Thirumany Sritharan,<sup>1, #</sup>  
Subodh Mhaisalkar,<sup>1, #</sup> Ming-Yong Han,<sup>‡</sup> Dan Wang,<sup>\*, §</sup> and Hongyu Chen<sup>\*, †, #</sup>*

<sup>†</sup>Division of Chemistry and Biological Chemistry, Nanyang Technological University, 21 Nanyang Link,  
Singapore 637371

<sup>§</sup>State Key Laboratory of Multi-phase Complex Systems, Institute of Process Engineering, Chinese  
Academy of Sciences, Beijing 100190, P. R. China

<sup>1</sup>School of Materials Science and Engineering, Nanyang Technological University, 50 Nanyang Avenue,  
Singapore, 639798

<sup>‡</sup>Institute of Materials Research and Engineering, Agency for Science, Technology and Research, 3  
Research Link, Singapore 117602

<sup>#</sup>Singapore-Berkeley Research Initiative for Sustainable Energy, 1 Create Way, Singapore 138602.

Email: [hongyuchen@ntu.edu.sg](mailto:hongyuchen@ntu.edu.sg); Web: <http://www.ntu.edu.sg/home/hongyuchen/>

**Preparation of TEM Samples.** TEM grids were treated with oxygen plasma in a Harrick plasma cleaner/sterilizer for 45 s to improve the surface hydrophilicity. The hydrophilic face of the TEM grid was then placed in contact with the sample solution. A filter paper was used to wick off the excess solution on the TEM grid, which was then dried in air for 5 min.

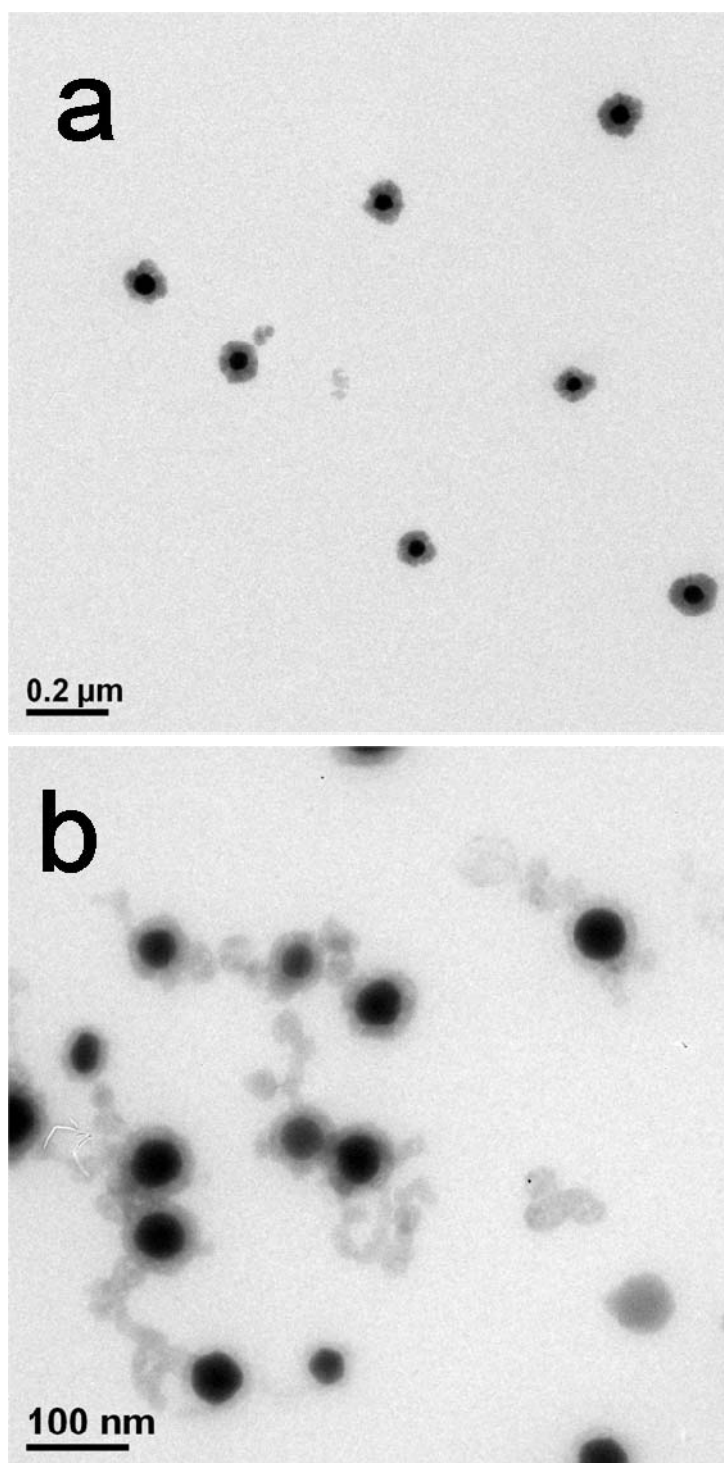


**Figure S1.** TEM images of the Au@ZnO core-shell NPs prepared from (a)  $\text{Zn}(\text{CH}_3\text{COO})_2$  and HMTA, and (b)  $\text{Zn}(\text{NO}_3)_2$  and  $\text{Na}_2\text{CO}_3$ .

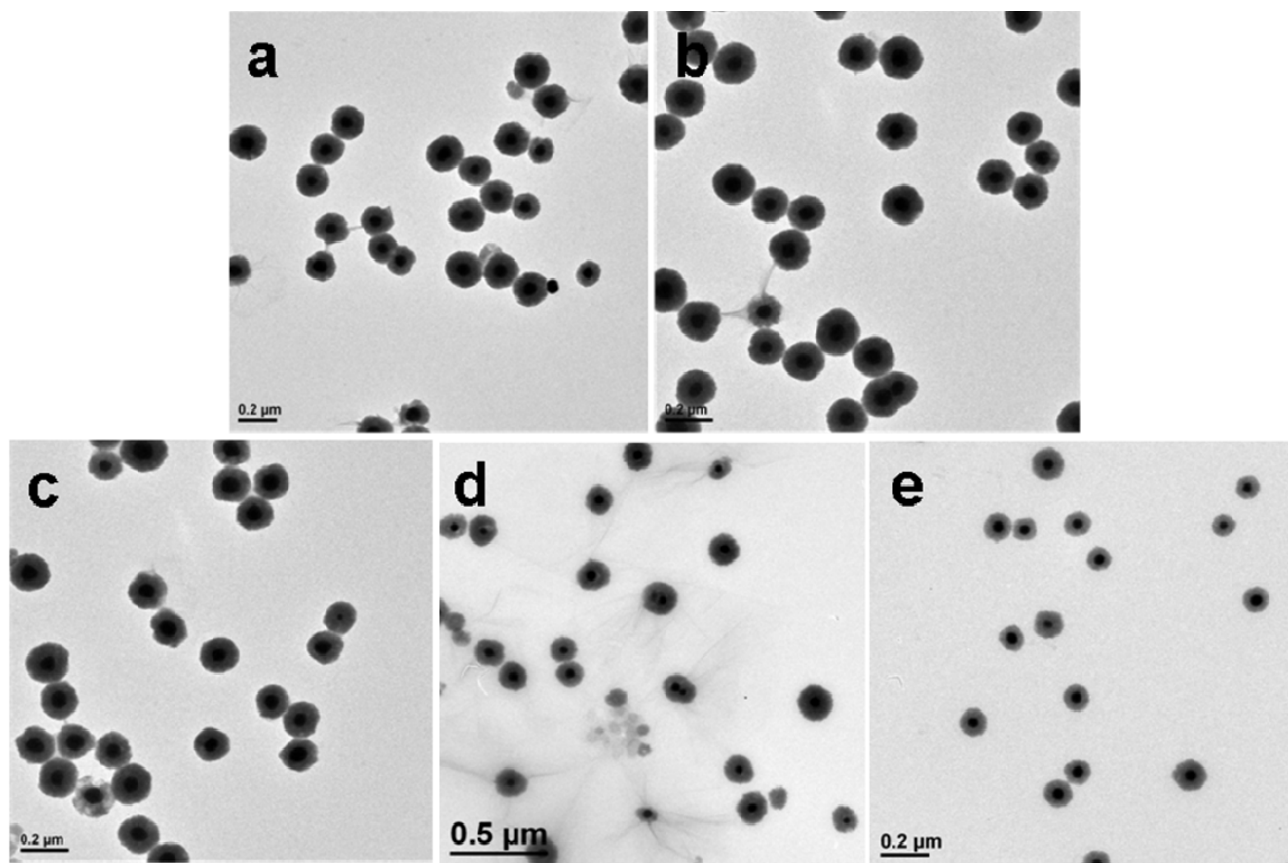


**Figure S2.** TEM images of the Au@ZnO core-shell NPs prepared in the presence of PVP from Au seeds modified with different ligands: (a) mercaptoacetic acid (ligand **2**), (b) 11-mercaptopundecanoic acid (ligand **3**), (c) 4-ethylthiophenol (ligand **5**) (d) 1-octadecanethiol (ligand **6**), and (e) 2-dipalmitoyl-sn-glycero-3-phosphothioethanol (sodium salt) (ligand **7**).

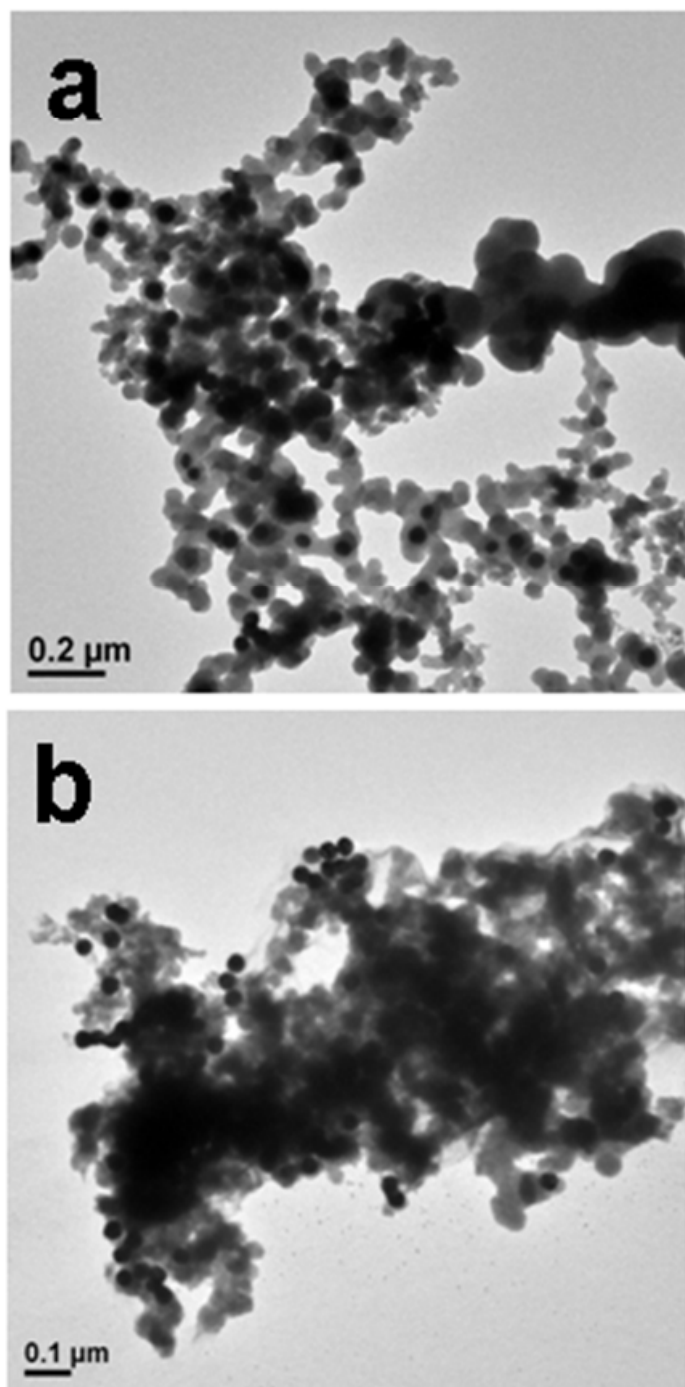


**Figure S3.** TEM images of the Au/ZnO hybrids prepared in the absence of PVP from Au seeds modified with (a) 11-mercaptopundecanoic acid (ligand **3**) and (b) 2-dipalmitoyl-*sn*-glycero-3-phosphothioethanol (sodium salt) (ligand **7**).

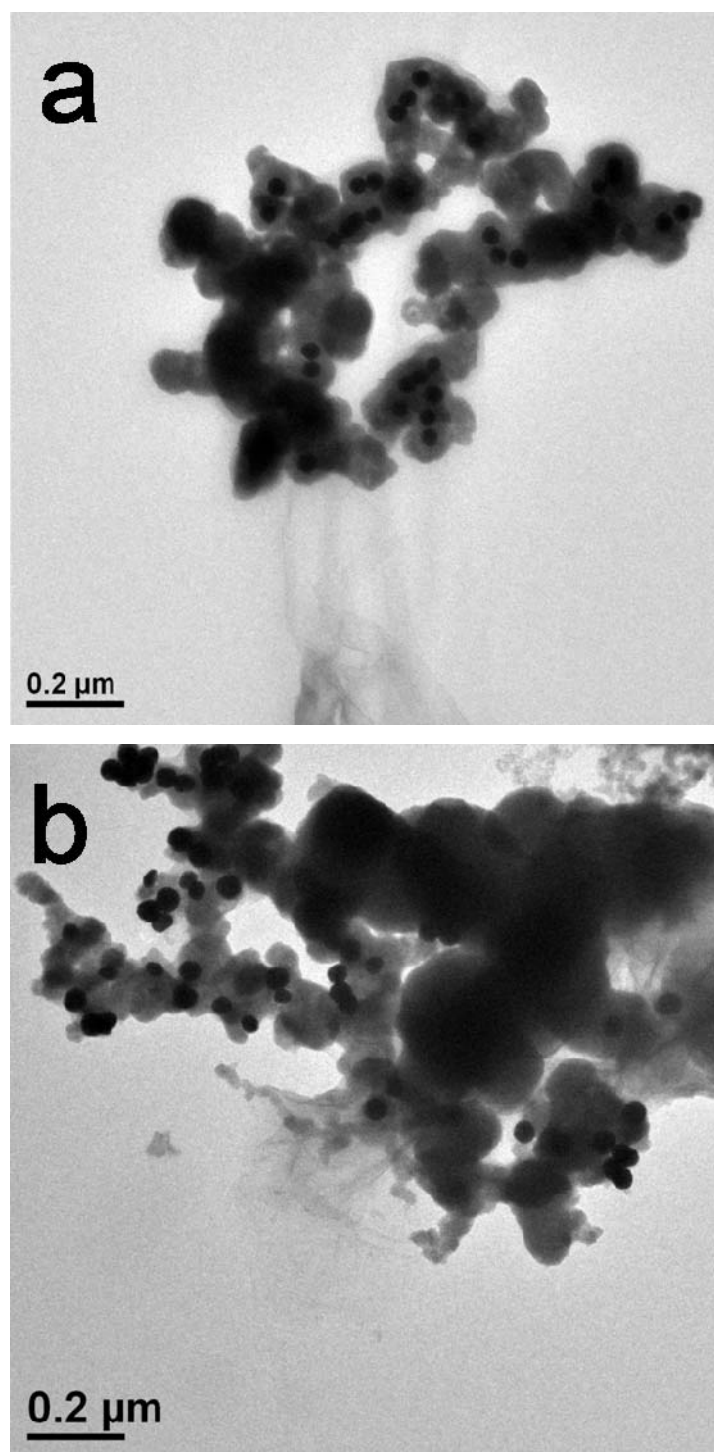


**Figure S4.** TEM images of the Au/ZnO hybrids prepared in the presence of PEG from Au seeds modified with different ligands: (a) 4-mercaptobenzoic acid (ligand **1**) and (b) 2-naphtalenethiol (ligand **4**).

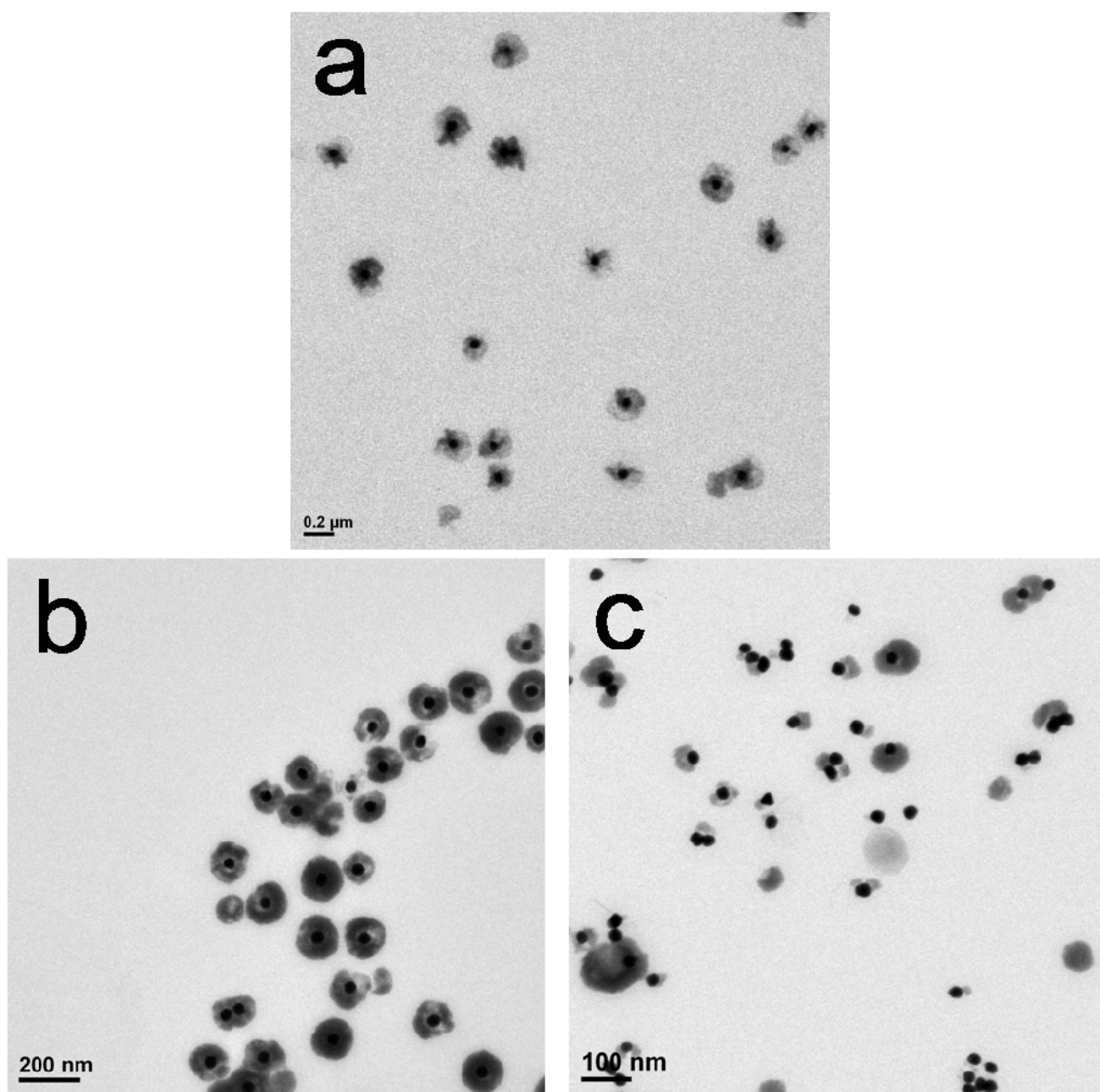


**Figure S5.** PVP incorporation in ZnO. Using high molecular weight PVP (360,000), the segregated PVP domains in the Au@ZnO NPs can be directly observed in the TEM images: (a) 4-mercaptopbenzoic acid (ligand **1**) and (b) 2-naphtalenethiol (ligand **4**), and (c) no ligand was used.

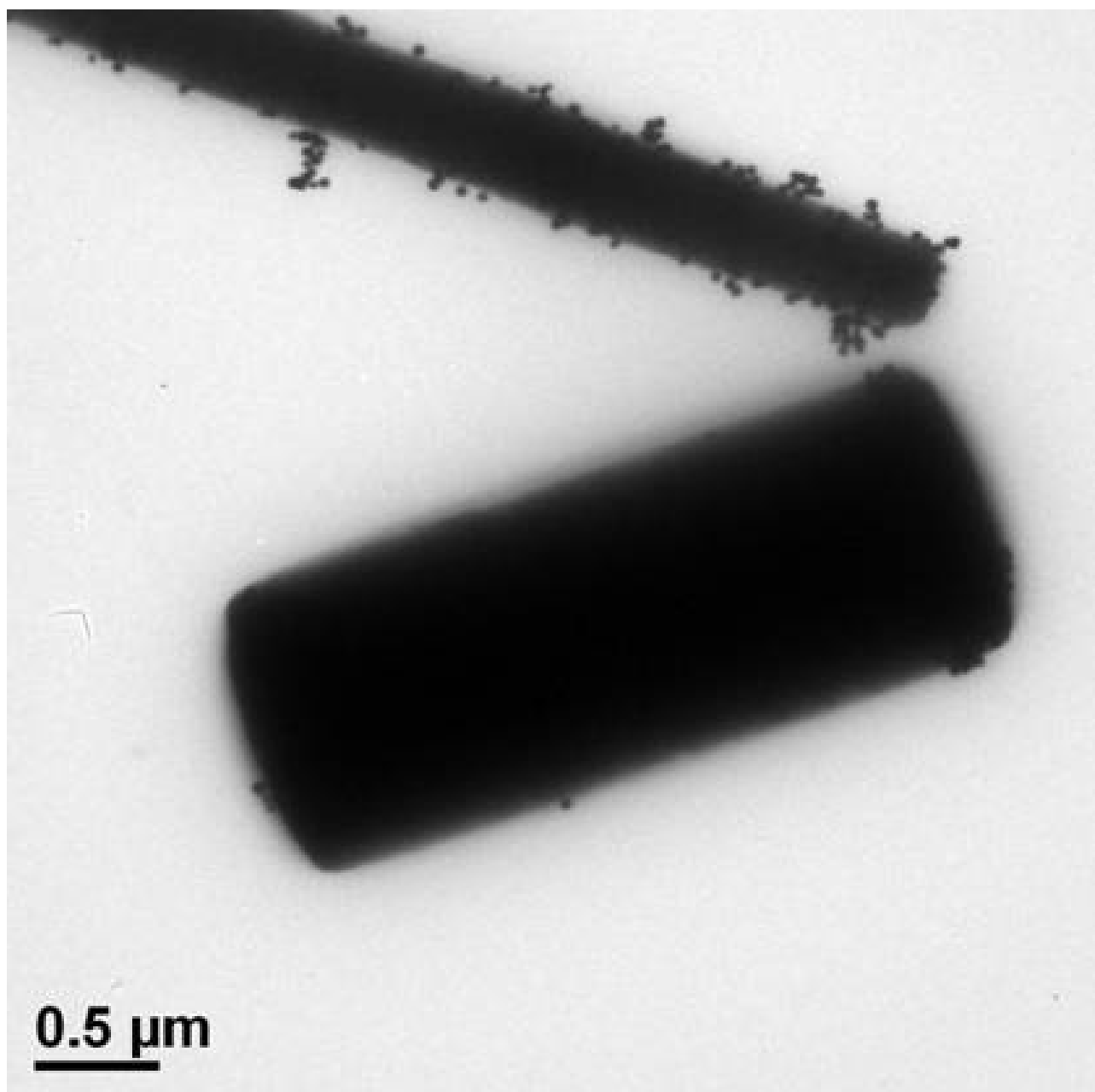


**Figure S6.** TEM image of Au/ZnO nanohybrid prepared in the absence of PVP and ligand.



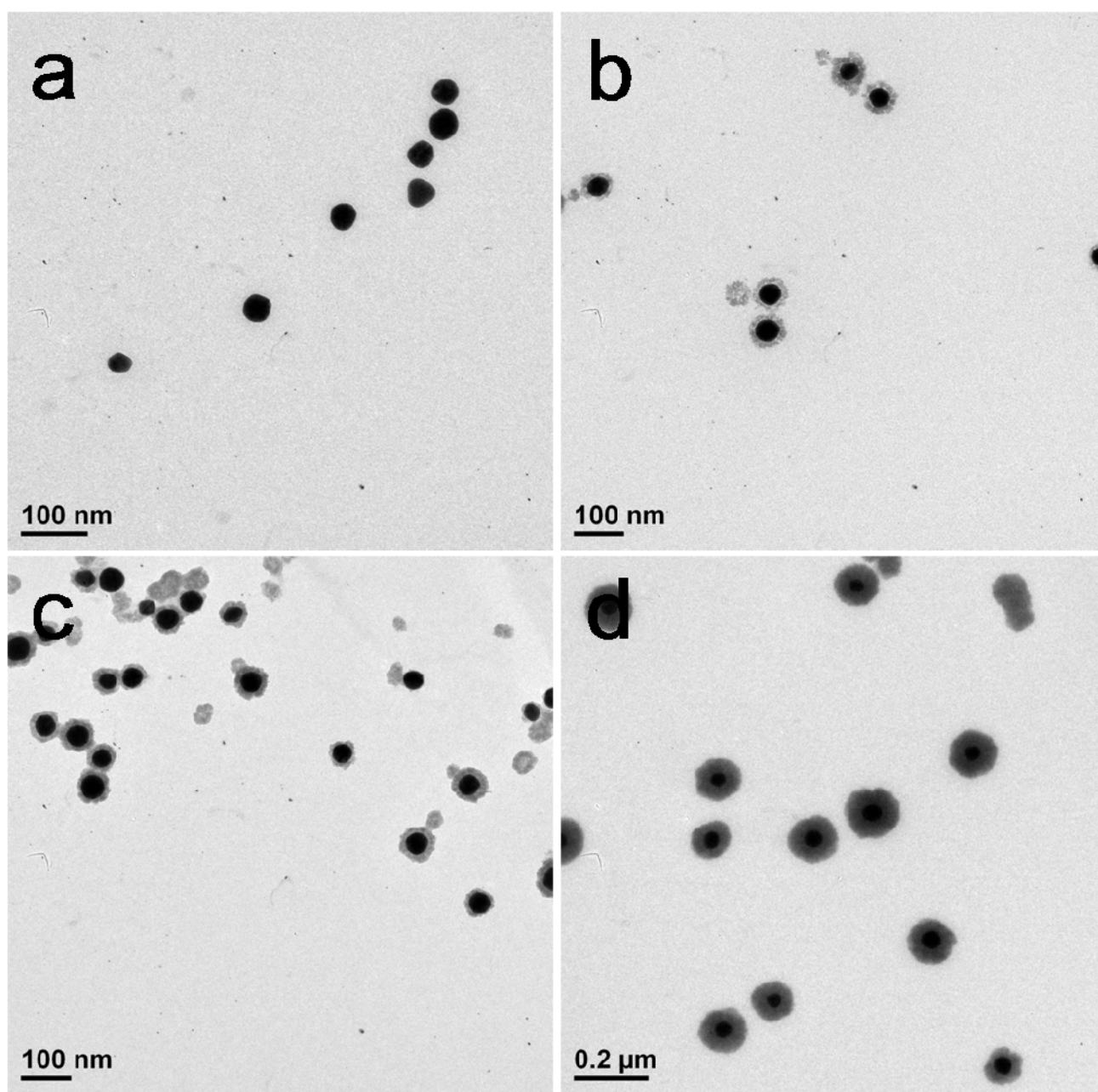


**Figure S7.** TEM images of temporal evolution of Au@ZnO core-shell NPs: (a)  $t = 10$  min, (b)  $t = 20$  min, (c)  $t = 30$  min, and (d)  $t = 1$  h.

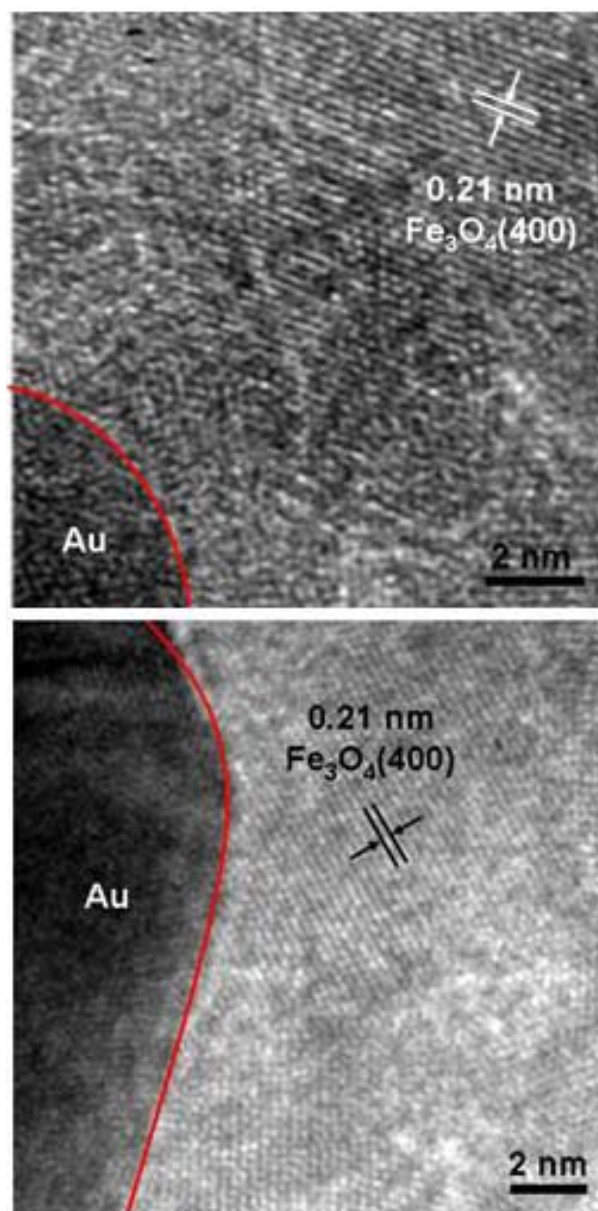


**Figure S8.** HRTEM images of the Au@Fe<sub>3</sub>O<sub>4</sub> core-shell NPs. The lattice spacing was measured as 0.21 nm, consistent with the (400) plane of Fe<sub>3</sub>O<sub>4</sub> lattice.

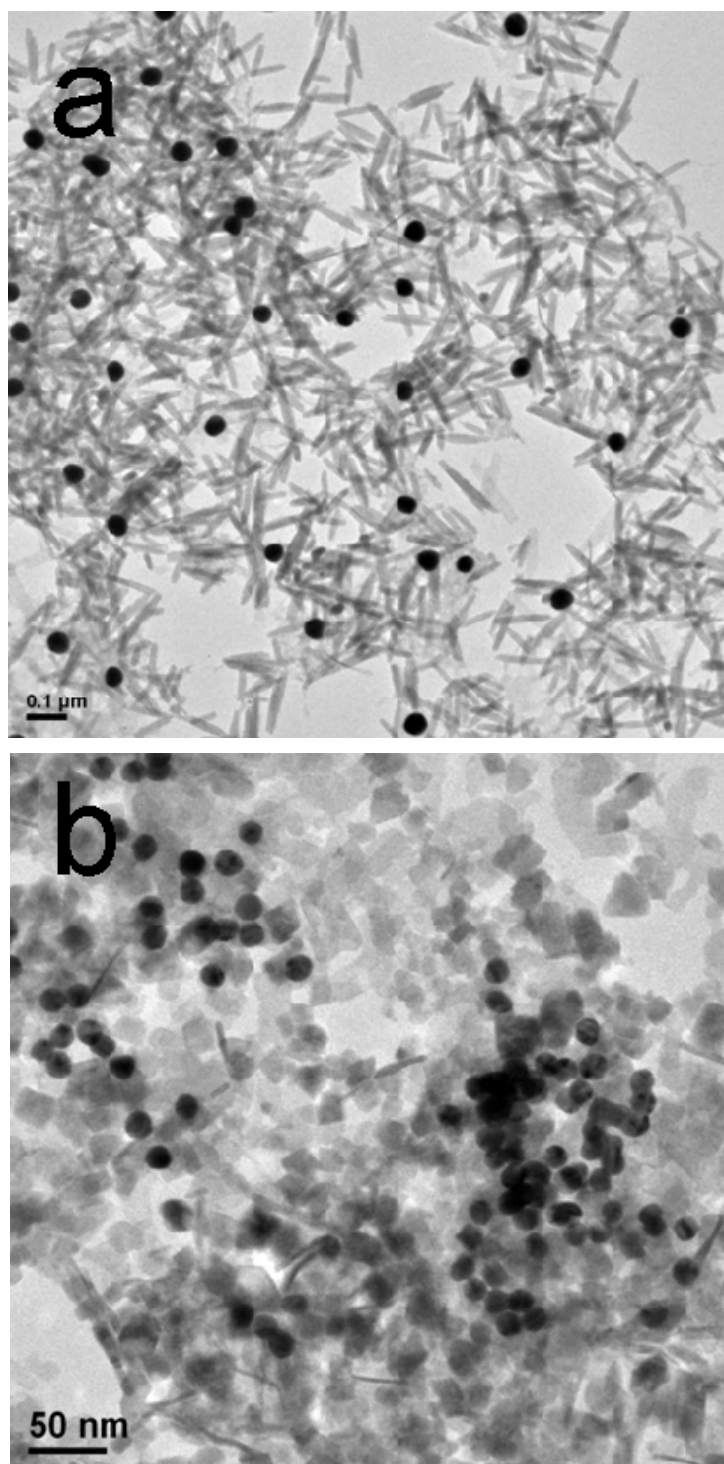


**Figure S9.** TEM images of (a) Au/ $\text{Fe}_2\text{O}_3$  hybrid prepared from  $\text{FeCl}_3$  and HMTA and (b) Au/ $\text{MnO}$  hybrid prepared from  $\text{MnCl}_2$  and HMTA.

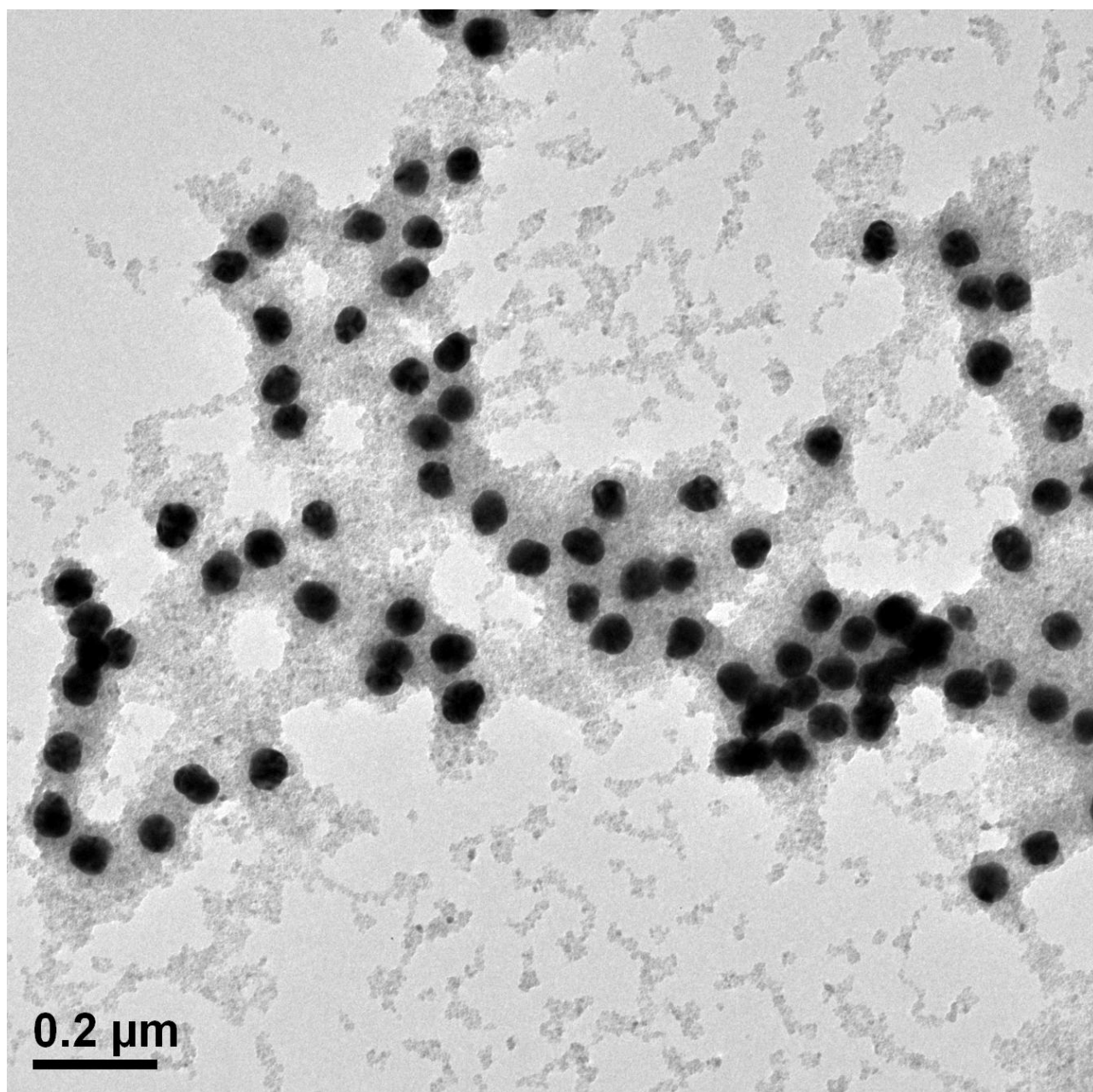


**Figure S10.** TEM image of Au/TiO<sub>2</sub> hybrid prepared from TiF<sub>4</sub> and HCl in the aqueous solution.

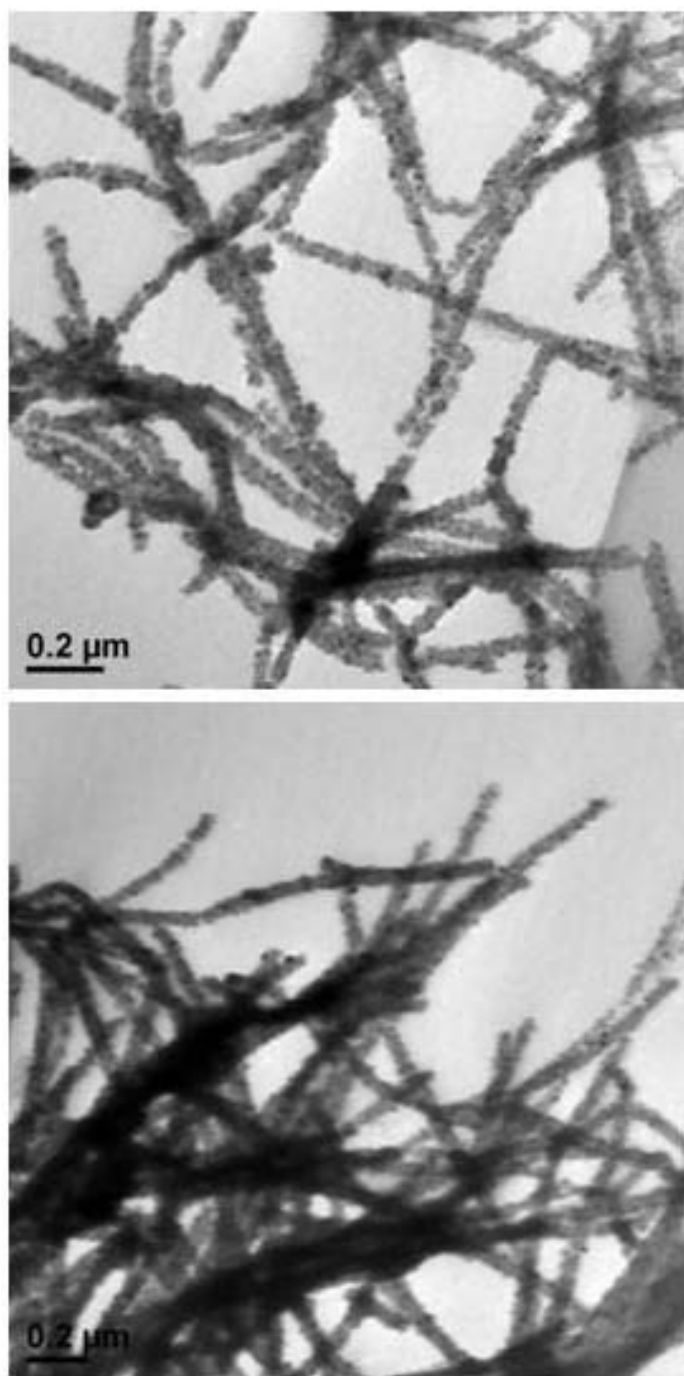


**Figure S11.** Two TEM images of CNT@CdS nanocomposites.



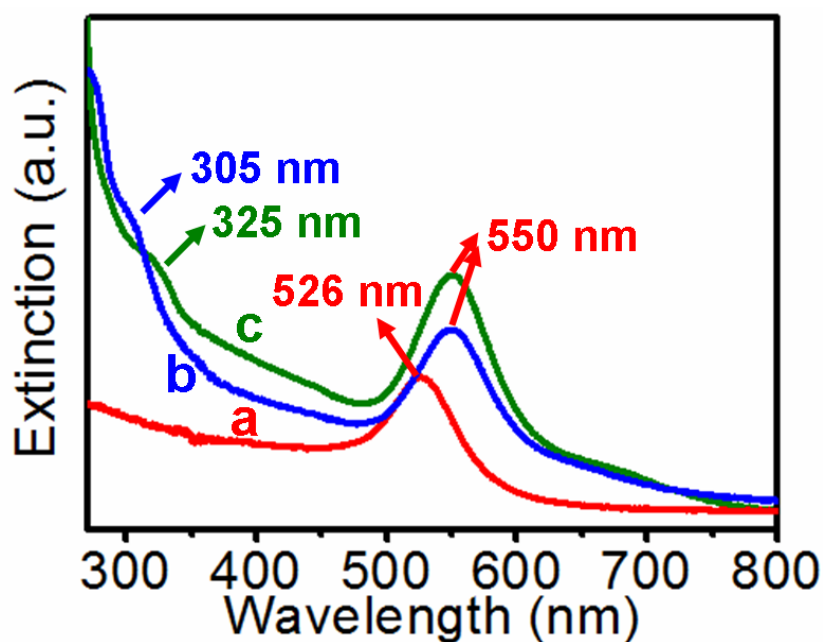


**Figure S12.** Optical-extinction spectral of (a) citrate-stabilized AuNPs (40 nm), (b) as-prepared Au@ZnO core-shell NPs, (c) Au@ZnO core-shell NPs after incubating in DMF (140 °C, 12 h).

The localized-surface-plasmon-resonance (LSPR) peak of Au@ZnO core-shell NPs shifts to ca. 550 nm (**Figure S12b,c**) from the original 526 nm of citrate-stabilized AuNPs (**Figure S12a**). These red-shifts arose due to an overall increase in the refractive index of the dielectric environment surrounding the AuNPs upon ZnO coating. Moreover, the as-prepared Au@ZnO core-shell NPs exhibit a ZnO excitonic peak at 305 nm (**Figure S12b**), which is blue shifted compared to bulk ZnO at 373 nm. It is noted that the ZnO shell in our case is included PVP modifier, and this blue shift in the ZnO/PVP samples have already been reported by other researcher.<sup>1</sup> Furthermore, the quantum confinement and/or deformed lattice of ZnO shell due to its polycrystalline nature may also contribute to this blue shift.<sup>2</sup> This excitonic peak red shifts from 305 nm to 325 nm after incubating Au@ZnO core-shell NPs in DMF (140 °C) for 12 h (**Figure S12c**), which improves the crystal quality of the ZnO shell.

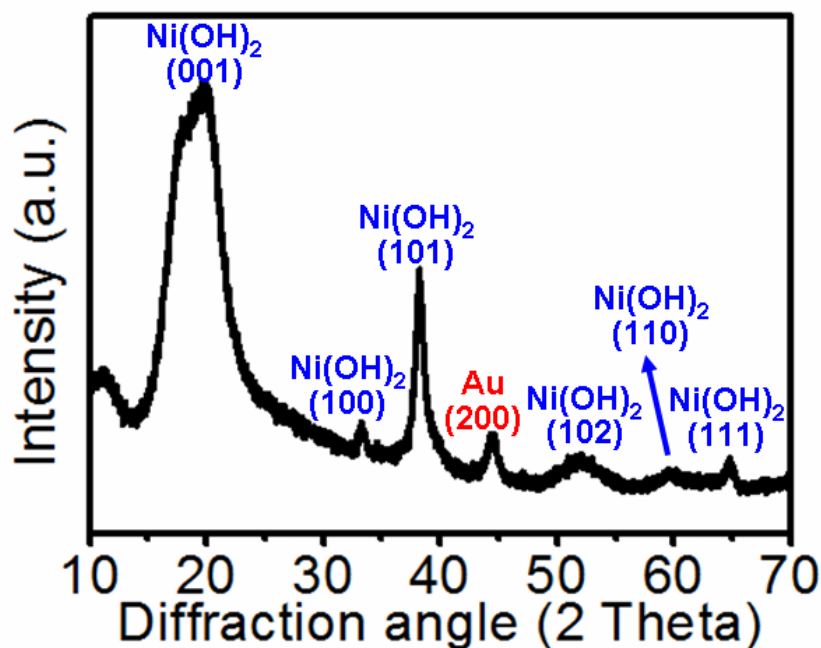


**Figure S13.** XRD pattern of Au@  $\beta$ -Ni(OH)<sub>2</sub> core-shell NPs.

XRD pattern agreed with the (001), (100), (101), (102), (110), (111) planes of hexagonal  $\beta$ -Ni(OH)<sub>2</sub> structure ( $a = 0.3126$  nm,  $c = 0.4605$  nm, JCPDS file No. 14-0117).<sup>3</sup> The remaining peak could be indexed to the face-centered-cubic Au (200) plane. Thus, the composition of the shell is hexagonal structured  $\beta$ -Ni(OH)<sub>2</sub>.

(1) Yao, K. X.; Zeng, H. C. *J. Phys. Chem. C* **2007**, *111*, 13301.

(2) Zhou, T.; Lu, M.; Zhang, Z.; Gong, H.; Chin, W. S.; Liu, B. *Adv. Mater.* **2010**, *22*, 403.

(3) Wang, Y.; Zhu, Q.; Zhang, H. *Chem. Commun.* **2005**, 5231.